

Stable periodic density waves in dipolar Bose-Einstein condensates trapped in optical lattices

Aleksandra Maluckov¹, Goran Gligorić^{2,3}, Ljupčo Hadžievski³, Boris A. Malomed⁴, and Tilman Pfau⁵

¹*Faculty of Sciences and Mathematics, University of Niš, P. O. B. 224, 18000 Niš, Serbia*

²*Max-Planck-Institut für Physik komplexer Systeme,
Nöthnitzer Straße 38, D-01187 Dresden, Germany*

³*Vinča Institute of Nuclear Sciences, University of Belgrade, P. O. B. 522, 11001 Belgrade, Serbia*

⁴*Department of Physical Electronics, School of Electrical Engineering,
Faculty of Engineering, Tel Aviv University, Tel Aviv 69978, Israel*

⁵*Physikalisches Institut, Universität Stuttgart, Pfaffenwaldring 57, 70569 Stuttgart, Germany*

Density-wave patterns in (quasi-) discrete media with local interactions are known to be unstable. We demonstrate that *stable* double- and triple- period patterns (DPPs and TPPs), with respect to the period of the underlying lattice, exist in media with nonlocal nonlinearity. This is shown in detail for dipolar Bose-Einstein condensates (BECs), loaded into a deep one-dimensional (1D) optical lattice (OL), by means of analytical and numerical methods in the tight-binding limit. The patterns featuring multiple periodicities are generated by the modulational instability of the continuous-wave (CW) state, whose period is identical to that of the OL. The DPP and TPP emerge via phase transitions of the second and first kind, respectively. The emerging patterns may be stable provided that the dipole-dipole (DD) interactions are repulsive and sufficiently strong, in comparison with the local repulsive nonlinearity. Within the set of the considered states, the TPPs realize a minimum of the free energy. Accordingly, a vast stability region for the TPPs is found in the parameter space, while the DPP stability region is relatively narrow. The same mechanism may create stable density-wave patterns in other physical media featuring nonlocal interactions, such as arrayed optical waveguides with thermal nonlinearity.

PACS numbers: 03.75.Lm; 05.45.Yv

Introduction. The formation of density-wave patterns in periodically structured media is a fundamental physical effect, celebrated manifestations of which are the Peierls instability of the electron gas in one-dimensional (1D) metals, leading to the emergence of charge-density waves [1, 2], and spin-density waves [2]. Recently, many complex settings known in solid-state physics have been reproduced (*simulated*) in an essentially simpler form in quantum gases—often, these are atomic Bose-Einstein condensates (BECs)—loaded into optical lattices (OLs) [3]. Thus far, this possibility was not demonstrated for density-wave patterns, the reason being that such patterns formed in BEC with contact interactions between atoms are unstable [4]. The objective of this work is to demonstrate that *stable* density waves are possible in BEC with long-range dipole-dipole (DD) inter-atomic interactions. The same mechanism should make it possible to create stable density (intensity) waves in other periodically structured physical media featuring a nonlocal nonlinear response, which is inherently present in the transport mechanisms of heat [5] and charge carriers [6], electrostatic interactions in liquid crystals [7], photon self-attraction [8], and many-body interactions in plasmas [9] and BEC [10]. Further, an effective gravitation-like attraction between atoms can be optically induced in BEC by means of resonant illumination [11]. It was demonstrated theoretically [12] and experimentally [13] that the implementation of patterns supported by the nonlocal nonlinearity is especially relevant in thermal optical media, where the periodic structure can be readily built in the form of arrayed waveguiding systems.

BEC of dipolar atoms or molecules loaded into OLs have been in the focus of research work for the past decade, starting from the theoretical analysis of basic properties of such condensates [14], followed by the analysis of quantum phases [15, 16], various textures [17, 18], and suppression of the quantum collapse (fall onto an attractive center) [19] in them. Structured ground states and supersolidity of dipolar gases [14, 20, 21], as well as the rotonic dispersion relation [22], were discussed theoretically but still await experimental confirmation. Experimentally, first effects of dipolar interactions in quantum gases were observed in the BEC of ⁵²Cr atoms [23]. A condensate of ¹⁶⁴Dy atoms was recently created too [24], which provides an even stronger DD interaction than ⁵²Cr. In addition to that, the creation of dipolar BEC is expected in erbium [25] and in gases of molecules carrying electric dipole moments [26]. A powerful tool which allows one to control dynamical effects in the dipolar BEC, such as the onset of collapse, is the use of the Feshbach resonance for tuning the strength of contact interactions between atoms, which compete with their long-range DD interactions [27]. The results obtained in this field have been summarized in recent review [28].

Another ubiquitous tool used in experiments with dipolar BEC is provided by OLs. Recently, dipolar effects in the chromium condensate trapped in OLs were reported in Refs. [29–31]. In particular, strong DD repulsion can stabilize the condensate with attractive contact interactions, trapped in the OL [31]. It is well known that the OL facilitates the creation of gap solitons [32], or bound pairs of repulsively interacting atoms, at the microscopic level [33]. Gap

solitons in the 1D model of dipolar condensates trapped in the OL potentials were studied in Ref. [34].

While the state of the trapped condensate may obviously feature the same periodicity as the underlying lattice (we call it the continuous-wave state, CW), we here report *stable* density waves in the form of double- and triple-period patterns (DPPs and TPPs) in the dipolar BEC loaded into a deep OL potential. The TPP realizes a relatively deep energy minimum in the space of the considered states, and its stability area is much broader than that of the DPP, therefore the TPP is a candidate to the role of the ground state. To the best of our knowledge, this is the first demonstration of stable density waves of the TPP type in OL-trapped BECs, as well as in dynamical lattices with long-range interactions of any physical nature. Featuring long-range off-diagonal and diagonal order different from that of the underlying lattice potential, both the DPPs and TPPs may be viewed as a metastable supersolid state [20, 21, 35] of the dipolar condensate.

In Ref. [4] it was demonstrated that the period-doubling instability of the CW in the BEC with local interactions, trapped in the deep OL, gives rise to DPPs, but, as mentioned above, the emerging pattern is *never* stable. As for the TPPs, an incentive for their consideration is provided by the recent analysis of the trapped dipolar BEC, which concluded that a three-well system is the minimal setting which is necessary to let the nonlocal character of the DD interactions manifest itself [18]. In this work we consider all possible combinations of the repulsive/attractive contact (RC/AC) and repulsive/attractive DD (RDD/ADD) interactions, and demonstrate that *unstaggered* (regular) DPPs and TPPs have their *stability regions* in the RC+RDD case, provided that the long-range DD repulsion is sufficiently strong in comparison with the local self-repulsion (these findings imply that, in the opposite AC+ADD case, the *staggered* [36] counterparts of these patterns are stable in the respective regions too). The analysis reveals that the multiple-period patterns emerge when the corresponding modulational instability of the CW sets in, i.e., the respective perturbations seed the creation of the patterns. The TPP's stability area is found to be much larger than that of the DPP, and the calculation of the free-energy density demonstrates that the TPP realizes a well-pronounced energy minimum, in comparison with the CW and DPP states. When the TPPs are unstable, the DD interactions of either sign significantly inhibits the instability, suggesting that even unstable TPPs may be observed in the experiment.

The model. For condensates loaded into a deep OL, the corresponding Gross-Pitaevskii equation can be reduced to the discrete nonlinear Schrödinger equation (DNLSE) in the framework of the tight-binding approximation [4, 37] (a similar reduction to the quasi-discrete propagation is well known in optics [38]). In turn, the analysis of various stationary states supported by the DNLSE may start from the anti-continuum limit, which corresponds to the chain of uncoupled sites [39]. The same tight-binding approximation, if applied to the dipolar BEC loaded into a deep OL, leads to the 1D [15, 40] and 2D [41] DNLSEs which include the long-range DD interaction between lattice sites. We here consider the trapped condensate modeled by the scaled 1D equation [40]:

$$i\frac{df_n}{dt} = -C(f_{n+1} + f_{n-1} - 2f_n) + \sigma |f_n|^2 f_n - \Gamma \sum_{m \neq n} \frac{|f_m|^2}{|m-n|^3} f_n, \quad (1)$$

where $\sigma = -1$ and $+1$ corresponds to the attractive and repulsive contact interaction, respectively, $C > 0$ is the inter-site coupling constant which accounts for the tunneling of atoms between adjacent sites of the lattice, and $\Gamma > 0$ or $\Gamma < 0$ is the relative strength of the DD attraction or repulsion, in comparison to the local nonlinearity. In fact, σ accounts for the *effective* on-site nonlinearity, which includes both the DD interaction between atoms trapped in a given potential well and the contact interaction proper. Time is measured in units of ω_\perp^{-1} , where ω_\perp is the frequency which defines the radius of the transverse confinement, $a_\perp = \sqrt{\hbar/(m_{\text{atom}}\omega_\perp)}$. C may also be fixed by rescaling, therefore basic findings are displayed below for $C = 0.8$. In this work, we present results for unstaggered patterns. They can be made equivalent to their staggered counterparts by transformation $f_n \rightarrow (-1)^n e^{4iCt} f_n^*$, $\{\sigma, \Gamma\} \rightarrow -\{\sigma, \Gamma\}$.

Equation (1) does not include the external trapping potential. Under realistic experimental conditions, the actual number of OL periods in the trap is $\gtrsim 100$. It is straightforward to check that distortion introduced by this potential is negligible for the patterns reported below. Undistorted configurations can also be realized in the dipolar condensate loaded into a toroidal trap [42].

For other nonlocal systems, such as optical media with the thermal nonlinearity [12], the DNLSE differs by the form of the kernel accounting for the long-range interaction. Essentially the same analysis as reported below can be developed for such models too.

Stationary solutions to Eq. (1) with chemical potential μ are sought for as $f_n = U_n \exp(-i\mu t)$, which leads to the equation for real discrete wave function U_n :

$$\mu U_n = -C(U_{n+1} + U_{n-1} - 2U_n) + \left[\sigma U_n^2 - \Gamma \sum_{m \neq n} \frac{U_m^2}{|m-n|^3} \right] U_n. \quad (2)$$

First, a straightforward analysis of the modulational instability of the unstaggered CW (constant) solution, $U_n^2 \equiv \mu/[\sigma - 2\zeta(3)\Gamma]$, where $\zeta(3) \approx 1.202$ is the zeta-function, has been performed, using the linearization of Eq. (1) for

small perturbations. In the most relevant RC+RDD case, the CW is stable in a relatively narrow parameter region, see Fig. 1.

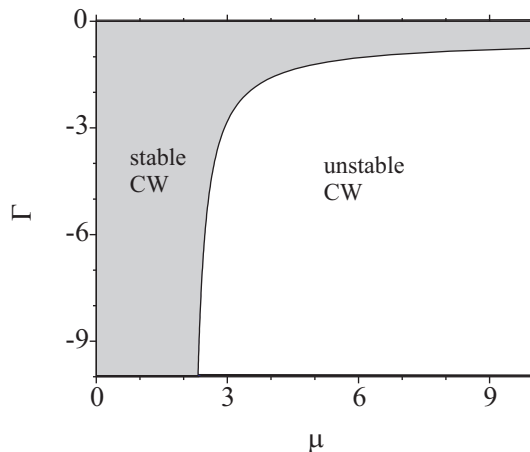


FIG. 1: The stability diagram for unstagged CW states with the repulsive sign of both the contact and DD interactions ($\sigma = +1, \Gamma < 0$). In all figures, the lattice coupling constant is $C = 0.8$.

Stable double-period and triple-period patterns. The formation of multiple-period patterns is a consequence of the modulational instability of the CW states, which represent uniform chains of BEC droplets trapped in the OL. Accordingly, periodically modulated patterns may be called *condensate-density waves*. They were found numerically by solving Eqs. (2) with the help of the modified Powell method [40], and also in exact and approximate analytical forms (see below). Their stability was explored by computing eigenvalues for small perturbations, using the linearization of Eq. (1), which was then checked by direct simulations of Eq. (1) for perturbed solutions. Close to the anticontinuum limit, patterns with all periodicities are long-lived ones, as the instability weakens with the decay of the inter-site coupling. This is a generic property of the DNLS with the contact nonlinearity [36], which persists in the presence of the DD interaction.

DPPs which are shown in the top row of Fig. 2, with U_n taking two values, $\phi_1 \neq \phi_2$, can be found as exact solutions of Eq. (2):

$$\phi_1^2 + \phi_2^2 = 4 \frac{\mu - 2C}{4\sigma - \Gamma\zeta(3)}, \quad \phi_1\phi_2 = \frac{-4C}{2\sigma + 3\Gamma\zeta(3)}, \quad (3)$$

Figure 3(a) demonstrates that both the linear-stability analysis and direct simulations reveal a rather narrow stability area of the unstagged DPPs for the RC+RDD sign combination of the interactions. At large μ , the upper boundary of the region is determined by the positivity of $\phi_1\phi_2$ (i.e., the “unstaggerness” of the pattern) in Eq. (3) with $\sigma = +1$: $\Gamma < -2/(3\zeta(3)) \approx -0.55$. The DPP is created by the *supercritical* pitchfork bifurcation [43] (in other words, through the phase transition of the second kind) at $\mu_{\text{cr}} = 2C [4\Gamma\zeta(3) - 2\sigma] / [2\sigma + 3\Gamma\zeta(3)]$, which is found from Eq. (3) by setting $\phi_1 = \phi_2$. At the bifurcation point, the DPP branch may emerge as a stable one [Fig. 3(b)], or, at larger $|\Gamma|$, as an unstable solution, which quickly enters the stability region with the further increase of μ [Fig. 3(c)]. As seen in Fig. 3(c), in the latter case the CW solution becomes unstable against other perturbations at $\mu = \mu_1$, but it remains stable against the period-doubling perturbations up to $\mu = \mu_{\text{cr}}$.

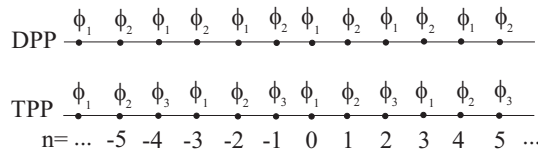


FIG. 2: A scheme of the condensate density waves with the double and triple periodicity. $\phi_{1,2,3}$ are amplitudes of the wave function at the lattice sites.

The TPPs are schematically shown in the bottom row of Fig. 2. Equations for the three real amplitudes, which are designated in the figure, are derived from Eq. (2):

$$\mu\phi_1 = -C(\phi_2 + \phi_3 - 2\phi_1) + \sigma\phi_1^3 - \Gamma\phi_1 (b\phi_1^2 + a(\phi_2^2 + \phi_3^2)), \quad (4)$$

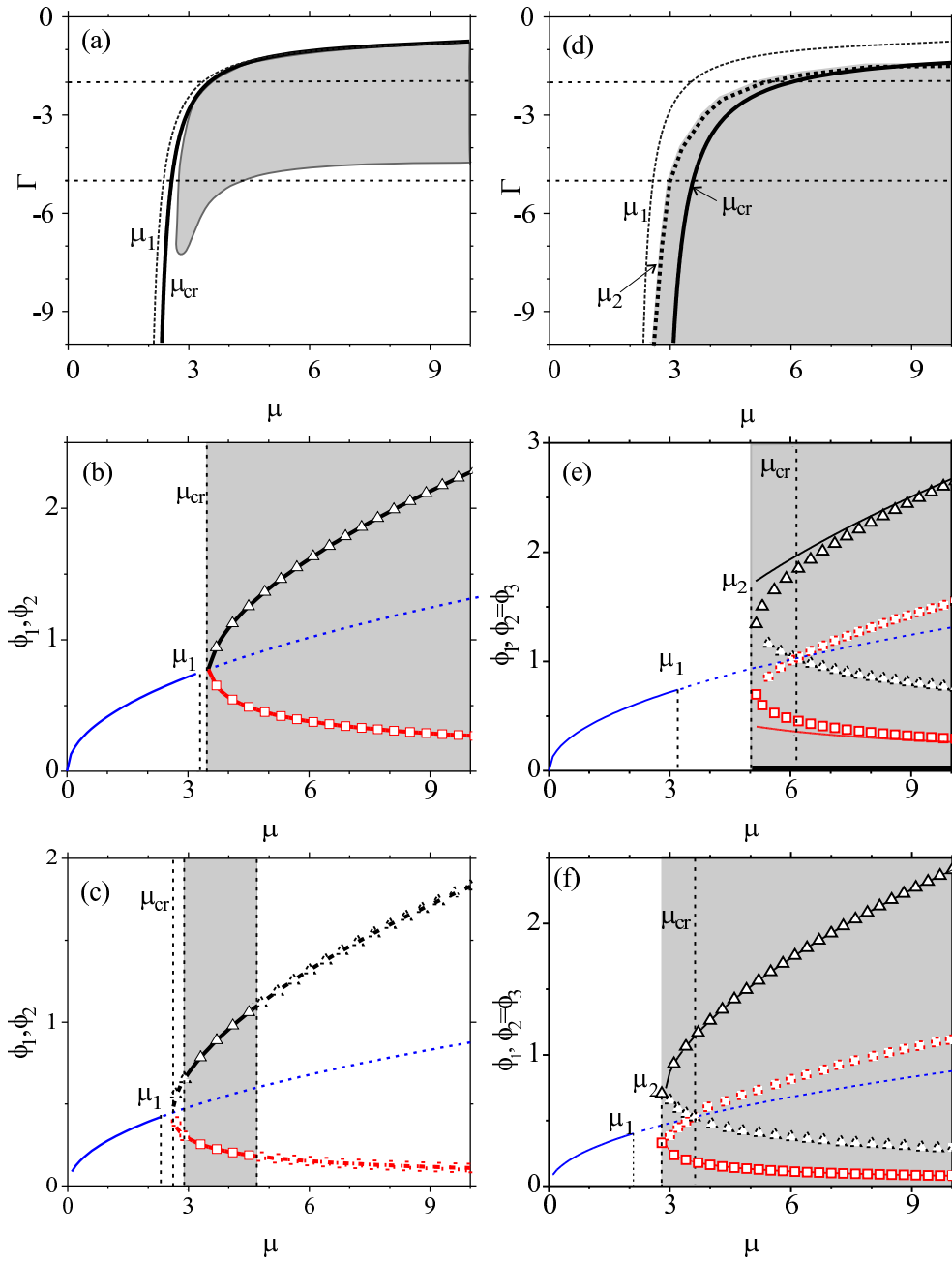


FIG. 3: (Color online) The stability diagram of the unstagged DPPs (a), and TPPs (d) for the RC+RDD interactions ($\sigma = +1, \Gamma < 0$). The DPPs (a)-(c) and TPPs (d)-(f) are stable in the gray area, while the dotted curve, $\mu = \mu_1(\Gamma)$, separates stability and instability regions (on its left and right sides) of CWs. The DPP is generated, via the pitchfork bifurcation, from the CW branch by period-doubling perturbations at $\mu = \mu_{cr}(\Gamma)$, which is marked by the solid curve in (a), while the stable TPP is generated by the subcritical pitchfork bifurcation at the turning point, $\mu = \mu_2 < \mu_{cr}$ (d)-(f). Amplitudes of the unstagged DPP and TPP are plotted vs. μ in (b),(c), and (e), (f) for $\Gamma = -2$ and $\Gamma = -5$, respectively [these values of Γ are marked in (a) and (d) by dashed horizontal lines]. Chains of symbols and continuous curves show, severally, numerical results and analytical solution for DPP (3) and TPP (5). The blue line (which seems as a bisector) represents the CW solution. Stable and unstable states are shown by solid and dashed lines or symbols, respectively.

and two other equations obtained by cyclic transpositions of $\{1, 2, 3\}$. Here, $a \equiv -[\psi(1/3) + \psi(2/3)]/54 \approx 1.157$ and $b \equiv 2\zeta(3)/27 \approx 0.089$, with $\psi(z) \equiv d[\ln(\Gamma(z))]/dz$. These equations give rise to three types of TPPs. *Type 1* is defined by assuming $\phi_2 = \phi_3 \ll \phi_1$, which yields an approximate analytical solution,

$$\phi_1 = \sqrt{\frac{\mu - 2C}{\sigma - \Gamma b}}, \quad \phi_2 = \phi_3 = \frac{-C}{\sigma + (a - b)\Gamma} \sqrt{\frac{\sigma - \Gamma b}{\mu - 2C}}. \quad (5)$$

Type 2 is similar to *Type 1*, but with comparable absolute values of the amplitudes: $\phi_1 > 0$, $\phi_2 = \phi_3 < 0$, and *Type 3* is an exact solution with $\phi_1 = 0$, $\phi_2 = -\phi_3 = \sqrt{(\mu - 3C)/[\sigma - \Gamma(a + b)]}$. The analysis demonstrates that solely *Type 1* may be stable, therefore only this type is considered below.

While the unstaggered TPPs exist for all combinations of the repulsive and attractive contact and DD interactions, only the RC+RDD combination gives rise to stable states, similar to the DPP. Again, the creation of the TPPs is related to properties of the CW background. As seen at Fig. 3(d), the CW becomes unstable against generic perturbations at $\mu = \mu_1$, but remains stable against the triple-period disturbances up to the bifurcation point, $\mu = \mu_{cr}$, which can be found exactly from Eq. (4): $\mu_{cr} = -(3C/2)[\sigma - (2a + b)\Gamma]/[\sigma + (a - b)\Gamma]$. A difference from the way the system gives rise to the stable DPP (see above) is that the bifurcation is (weakly) *subcritical* [43] in the present case (alias it is the phase transition of the first kind), with the stable TPP emerging by a jump at the turning point, $\mu = \mu_2 < \mu_{cr}$, see Figs. 3(e),(f).

All the varieties of unstaggered DPPs and TPPs are found to be entirely unstable for other types of the interactions, i.e., RC+ADD, AC+ADD, AC+RDD, with the instability growth rate increasing proportionally to the lattice coupling constant, C . On the other hand, at fixed C the instability growth rate *decreases* with the increase of the relative strength of the DD interactions (of either sign), which implies that they help to increase the lifetime of unstable density waves in the dipolar BEC. Direct simulations confirm the predictions of the linear-stability analysis, as well as the inhibition of the instability by the DD interactions.

A crucial issue is the comparison of energy of coexisting states. Considering spatially unconfined modes, controlled by the chemical potential, it is relevant to do this for the mean spatial density (g) of the corresponding free energy, $G \equiv H - \mu N$, where H and N are the Hamiltonian and number of atoms (norm of the wave function). The results, obtained analytically for the CW and DPP, and in a numerical form for the TPP, are shown in Fig. 4. For a large range of parameters the TPP is stable and realizes a relatively deep minimum of the energy, while the DPP may only represent a metastable state. Whether the TPP is the ground state, needs to be checked by comparing with more complex patterns, if they exist in the system. However even if it is a metastable configuration, it is relevant to explore its superfluid properties in further studies.

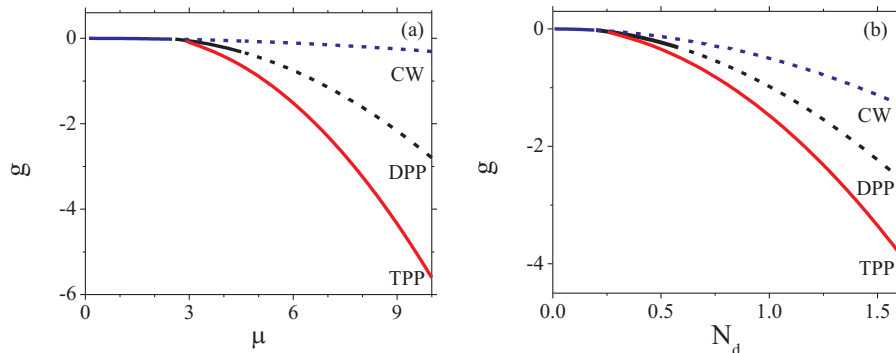


FIG. 4: (Color online) The free-energy density of the CW, DPP and TPP states vs. (a) the chemical potential and (b) atomic density, N_d , for $\sigma = +1$ and $\Gamma = -5$. The results are similar for other negative values of Γ .

As concerns parameters relevant to the experimental implementation of the stable condensate-density waves predicted here, in chromium the background s -wave scattering length is $a_s \sim 100a_B$. By means of the Feshbach resonance, it can be reduced to $\simeq 2a_B$, thus making the basic ratio $|\Gamma| = a_{DD}/a_s \gtrsim 5$, which is sufficient for getting into the stability areas displayed in Figs. 3(a) and 3(d). For the dipolar BEC of dysprosium and erbium, the collisional properties are not yet known in detail, but similar tuning options are expected. The creation of the DPP may not be straightforward, as it does not correspond to the energy minimum, unlike the TPP. To achieve this purpose, a periodic modulation of the lattice can be applied, cf. Refs. [44, 45]. As concerns the observation of the density-wave

patterns, in addition to direct imaging, their existence can be confirmed by measuring the momentum distribution in the time of flight, after switching off the potential.

Conclusion. Our analysis predicts stable density waves in OL-trapped dipolar BEC, and, as a matter of fact, in other periodically structured media with long-range interactions. In particular, the stable TPPs are predicted for the first time, to the best of our knowledge. The stability, which is limited to a relatively narrow region for the DPP, and is found in a broad area for the TPP, is provided by the long-range DD interactions, and is impossible in the BEC with solely the contact interactions. While the DPP is metastable, the TPP realizes a relatively deep energy minimum. These patterns emerge through the phase transitions of the second and first kinds, respectively. These condensate-density waves are bosonic counterparts of charge-density waves in 1D metals, created by the Peierls instability. The results suggest that the long-range DD interactions (whose effective strength in the quasi-1D setting can be adjusted by the direction of the polarizing magnetic field) may be used to steer transitions between different varieties of Mott-insulator states of the trapped bosons. The same mechanism may generate stable density waves in other physical settings—in particular, in optical media with nonlocal nonlinearities.

The findings reported here suggest a number of potentially interesting developments. A straightforward question is whether condensate density waves with periods larger than three may be stable. While this issue should be addressed by means of an accurate analysis, a simple estimate of the ways to minimize the energy of the system through the condensation of atoms at a relatively small number of the lattice sites suggests that patterns with higher values of the period may be favored by a still stronger contrast between the strengths of the DD and contact repulsion. An extension to multi-component condensates is interesting too. Further, Ref. [21], which recently reported a stable 2D checkerboard ground state in a related nonlocal model, suggests a possibility to search for stable density-modulation patterns in dipolar condensates trapped in a deep 2D OL, using the respective form of the DNLSE [41].

On the other hand, while the analysis in this work is restricted to the DNLSE model based on the “frozen” lattice, the DD interactions between condensate droplets trapped at local minima of the OL potential may distort the droplet chain, making it necessary to add another degree of freedom—a shift of the droplets from local potential minima. In a combination with the equation for the droplets’ mean-field wave function, this generalization may give rise to a new type of a dynamical system, blending the DNLSE with a model of the Frenkel-Kontorova type. Results obtained in the framework of such a coupled system will be reported elsewhere. Finally, it is interesting to extend the analysis to fermionic dipolar gases. In particular, it was very recently assumed that a Wigner crystal may emerge in a fermionic gas trapped in the OL [46].

Acknowledgments

A.M., G.G., and Lj.H. acknowledge support from the Ministry of Education and Science, Serbia (Project III45010). The work of B.A.M. and T.P. was supported in a part by the German-Israel Foundation (grant No. I-1024-2.7/2009).

-
- [1] R. E. Peierls, *Quantum Theory of Solids* (Oxford University Press: London, 1955).
 - [2] P. A. Lee, T. M. Rice, and P. W. Anderson, *Solid State Commun.* **14**, 703 (1974).
 - [3] M. Lewenstein, A. Sanpera, V. Ahufinger, B. Damski, A. Sen(De), and U. Sen, *Adv. Phys.* **56**, 243 (2007).
 - [4] M. Machholm, A. Nicolin, C. J. Pethick, and H. Smith, *Phys. Rev. A* **69**, 043604 (2004).
 - [5] S. A. Akhmanov, D. P. Krindach, A. V. Migulin, A. P. Sukhorukov, and R. V. Khokhlov, *IEEE J. Quantum Electron.* **4**, 568 (1968).
 - [6] E. A. Ulnatir, G. I. Stegeman, D. Michaelis, C. H. Lange, and F. Lederer, *Phys. Rev. Lett.* **90**, 253903 (2003).
 - [7] C. Conti, M. Peccianti, and G. Assanto, *Phys. Rev. Lett.* **91**, 73901 (2003).
 - [8] L. A. Rivlin, *Quantum Electron.* **28**, 99 (1998).
 - [9] H. L. Pécseli, and J. J. Rasmussen, *Plasma Physics Contr. Fusion* **22**, 421 (1980).
 - [10] F. Dalfovo, S. Giorgini, L. P. Pitaevskii, and S. Stringari, *Rev. Mod. Phys.* **71**, 463 (1999).
 - [11] D. O’Dell, S. Giovanazzi, G. Kurizki, and V. M. Akulin, *Phys. Rev. Lett.* **84**, 5687 (2000); S. Giovanazzi, D. O’Dell, and G. Kurizki, *Phys. Rev. A* **63**, 031603 (2001); I. Papadopoulos, P. Wagner, G. Wunner, and J. Main, *ibid.* **76**, 053604 (2007).
 - [12] W. Królikowski, O. Bang, J. J. Rasmussen, and J. Wyller, *Phys. Rev. E* **64**, 016612 (2001); O. Bang, W. Królikowski, J. Wyller, and J. J. Rasmussen, *ibid.* **66**, 046619 (2002); W. Królikowski, O. Bang, J. J. Rasmussen, and J. Wyller, *Opt. Exp.* **13**, 435 (2005).
 - [13] C. Rotschild, B. Alfassi, O. Cohen, and M. Segev, *Nature Physics* **2**, 769 (2006); A. Dreischuh, D. N. Neshev, D. E. Petersen, O. Bang, and W. Królikowski, *Phys. Rev. Lett.* **96**, 043901 (2006).
 - [14] K. Góral, K. Rzazewski and T. Pfau, *Phys. Rev. A*, **61**, 051601 (R) (2000); L. Santos, G. V. Shlyapnikov, P. Zoller and M. Lewenstein, *Phys. Rev. Lett.* **85**, 1791 (2000).
 - [15] K. Góral, L. Santos, and M. Lewenstein, *Phys. Rev. Lett.* **88**, 170406 (2002).

- [16] S. Yi, L. You, and H. Pu, Phys. Rev. Lett. **93**, 040403 (2004); Y. Kawaguchi, H. Saito, and M. Ueda, *ibid.* **97**, 130404 (2006); C. Menotti, C. Trefzger and M. Lewenstein, *ibid.* **98**, 235301 (2007); S. Ronen, D. C. E. Bortolotti and J. L. Bohn, *ibid.* **98**, 030406 (2007).
- [17] S. Yu and H. Pu. Phys. Rev. Lett. **97**, 020401 (2006); M. Vengalattore, S. R. Leslie, J. Guzman, and D. M. Stamper-Kurn, *ibid.* **100**, 170403 (2008); I. Tikhonenkov, B. A. Malomed, and A. Vardi, *ibid.* **100**, 090406 (2008); J. A. M. Huhtamäki, M. Takahashi, T. P. Simula, T. Mizushima, and K. Machida, Phys. Rev. A **81**, 063623 (2010).
- [18] T. Lahaye, T. Pfau, and L. Santos, Phys. Rev. Lett. **104**, 170404 (2010).
- [19] H. Sakaguchi and B. A. Malomed, Phys. Rev. A **83**, 013907 (2011); **84**, 033616 (2011).
- [20] S. Ronen, D. C. E. Bortolotti, and J. L. Bohn, Phys. Rev. Lett. **98**, 030406 (2007).
- [21] A. Bühler and H. P. Büchler, Phys. Rev. A **84**, 023607 (2011).
- [22] L. Santos, G. V. Shlyapnikov, and M. Lewenstein Phys. Rev. Lett. **90**, 250403 (2003).
- [23] A. Griesmaier, J. Werner, S. Hensler, J. Stuhler and T. Pfau, Phys. Rev. Lett. **94**, 160401 (2005); J. Stuhler, A. Griesmaier, T. Koch, M. Fattori, T. Pfau, S. Giovanazzi, P. Pedri and L. Santos, *ibid.* **95**, 150406 (2005); A. Griesmaier, J. Phys. B: At. Mol. Opt. Phys. **40**, 91 (2007).
- [24] M. Lu, S. H. Youn, and B. L. Lev, Phys. Rev. Lett. **104**, 063001 (2010); M. Lu, N. Q. Burdick, S. H. Youn, and B. L. Lev, preprint arXiv:1108.5993.
- [25] J. J. McClelland and J. L. Hanssen, Phys. Rev. Lett. **96**, 143005 (2006).
- [26] J. Deiglmayr, A. Grochola, M. Repp, K. Mörtlbauer, C. Glück, J. Lange, O. Dulieu, R. Wester, and M. Weidemüller, Phys. Rev. Lett. **101**, 133004 (2008); S. Ospelkaus, K.-K. Ni, G. Quémener, B. Neyenhuis, D. Wang, M. H. G. de Miranda, J. L. Bohn, J. Ye, and D. S. Jin, Phys. Rev. Lett. **104**, 030402 (2010).
- [27] T. Koch, T. Lahaye, J. Metz, B. Fröhlich, A. Griesmaier, and T. Pfau, Nature Physics **4**, 218 (2008).
- [28] T. Lahaye, C. Menotti, L. Santos, M. Lewenstein, and T. Pfau, Rep. Progr. Phys. **72**, 126401 (2009).
- [29] B. Pasquiou, G. Bismut, E. Maréchal, P. Pedri, L. Vernac, O. Gorceix, and B. Laburthe-Tolra, Phys. Rev. Lett. **106**, 015301 (2011).
- [30] M. Fattori, G. Roati, B. Deissler, C. D’Errico, M. Zaccanti, M. Jona-Lasinio, L. Santos, M. Inguscio, and G. Modugno, Phys. Rev. Lett. **101**, 190405 (2008).
- [31] S. Müller, J. Billy, E. A. L. Henn, H. Kadau, A. Griesmaier, M. Jona-Lasinio, L. Santos, and T. Pfau, <http://arxiv.org/abs/1105.5015>
- [32] V. A. Brazhnyi, and V. V. Konotop, Mod. Phys. Lett. B **18**, 627 (2004); O. Morsch and M. Oberthaler, Rev. Mod. Phys. **78**, 196 (2006).
- [33] K. Winkler, G. Thalhammer, F. Lang, R. Grimm, J. H. Denschlag, A. J. Daley, A. Kantian, H. P. Büchler, and P. Zoller, Nature Physics **4**, 04918 (2006).
- [34] J. Cuevas, B. A. Malomed, P. G. Kevrekidis, and D. J. Frantzeskakis, Phys. Rev. A **79**, 053608 (2009).
- [35] N. Prokof’ev, Adv. Phys. **56**, 381 (2007).
- [36] P. G. Kevrekidis, *The Discrete Nonlinear Schrödinger Equation: Mathematical Analysis, Numerical Computations, and Physical Perspectives* (Springer: Berlin and Heidelberg, 2009).
- [37] A. Trombettoni and A. Smerzi, Phys. Rev. Lett. **86**, 2353 (2001); Phys. Rev. A **68**, 023613 (2003); F. Kh. Abdullaev, B. B. Baizakov, S. A. Darmanyan, V. V. Konotop, and M. Salerno, Phys. Rev. A **64**, 043606 (2001); A. Smerzi, A. Trombettoni, P. G. Kevrekidis, and A. R. Bishop, Phys. Rev. Lett. **89**, 170402 (2002).
- [38] F. Lederer, G. I. Stegeman, D. N. Christodoulides, G. Assanto, M. Segev, and Y. Silberberg, Phys. Rep. **463**, 1 (2008).
- [39] S. Aubry, Physica D **103**, 201 (1997).
- [40] G. Gligorić, A. Maluckov, Lj. Hadžievski, and B. A. Malomed, Phys. Rev. A **78**, 063615 (2008); **79**, 053609 (2009).
- [41] G. Gligorić, A. Maluckov, M. Stepić, Lj. Hadžievski, and B. A. Malomed, *ibid.* **81**, 013633 (2010); **82**, 033624 (2010).
- [42] M. Abad, M. Guilleumas, R. Mayol, and M. Pi, Phys. Rev. A **81**, 043619 (2010); M. Abad, M. Guilleumas, R. Mayol, M. Pi, and D. M. Jezek, *ibid.* **84**, 035601 (2011); S. Zöllner, G. M. Bruun, C. J. Pethick, and S. M. Reimann, Phys. Rev. Lett. **107**, 035301 (2011).
- [43] G. Iooss and D. D. Joseph, *Elementary Stability and Bifurcation Theory* (Springer: New York, 1980).
- [44] N. Gemelke, E. Sarajlic, Y. Bidet, S. Hong, and S. Chun, Phys. Rev. Lett. **95**, 170404 (2005).
- [45] H. Lignier, C. Sias, D. Ciampini, Y. Singh, A. Zenesini, O. Morsch, and E. Arimondo, Phys. Rev. Lett. **99**, 220403 (2007).
- [46] Z. Xu and S. Chen, arXiv:1112.3419 (2011).